JOURNAL OF AGRICULTURAL AND FOOD CHEMISTRY

Agricultural and Environmental Chemistry

Discovery of Novel Thiazole Carboxamides as Antifungal Succinate Dehydrogenase Inhibitors

Xiaofeng Guo, Bin Zhao, Zhijin Fan, Dong-yan Yang, Nailou Zhang, Qifan Wu, Bin Yu, Shuang Zhou, Tatiana Kalinina, and Nataliya P. Belskaya

J. Agric. Food Chem., **Just Accepted Manuscript** • DOI: 10.1021/acs.jafc.8b06935 • Publication Date (Web): 23 Jan 2019

ACS Publications

is published by the American Chemical Society. 1155 Sixteenth Street N.W., Washington, DC 20036

Discovery of Novel Thiazole Carboxamides as Antifungal Succinate Dehydrogenase Inhibitors

Xiaofeng Guo[†], Bin Zhao*[,†], Zhijin Fan*[,†,‡], Dongyan Yang[†], Nailou Zhang[†], Qifan Wu[†], Bin Yu[†], Shuang Zhou[†], Tatiana A. Kalinina[§], Natalia P. Belskaya[§]

[†]State Key Laboratory of Elemento-Organic Chemistry, College of Chemistry, Nankai University, Tianjin 300071, P. R. China

[‡]Collaborative Innovation Center of Chemical Science and Engineering (Tianjin), Nankai University, Tianjin 300071, P. R. China.

[§]The Ural Federal University Named after the First President of Russia B. N. Yeltsin, Yeltsin UrFU 620002, Ekaterinburg, Russia.

* Address correspondence to these authors at State Key Laboratory of Elemento-Organic Chemistry, College of Chemistry, Nankai University, No. 94, Weijin Road, Nankai District, Tianjin 300071, P. R. China (telephone +86-13920714666; Fax:+86 022-23503620; e-mail: fanzj@nankai.edu.cn for Zhijin Fan or binzhao@nankai.edu.cn for Bin Zhao).

Abstract

To contribute molecular diversity for novel fungicide development, a series of novel thiazole carboxamides were rationally designed, synthesized and characterized with the succinate dehydrogenase (SDH) as target. Bioassay indicated that compound **6g** showed the similar excellent SDH inhibition as that of thifluzamide with IC_{50} of 0.56 mg/L and 0.55 mg/L, respectively. Some derivatives displayed improved *in vitro* fungicidal activities against *Rhizoctonia cerealis* and *Sclerotinia sclerotiorum* with EC_{50} of 1.2-16.4 mg/L and 0.5-1.9 mg/L, respectively, which was better than thifluzamide with its EC_{50} of 22.1 mg/L and 4.4 mg/L, respectively. Surprisingly, **6g** showed promising *in vitro* fungicidal activities against *R. cerealis* and *S. sclerotiorum* with EC_{50} of 6.2 and 0.6 mg/L, respectively, which was superior to thifluzamide with the EC_{50} of 22.1 and 4.4 mg/L, respectively. Additionally, compounds **6c** and **6g** displayed excellent *in vivo* fungicidal activities against *S. sclerotiorum* on *Brassica napus* L. leaves with protective activity of 75.4% and 67.3% at 2.0 mg/L, respectively, while thifluzamide without activity at 5.0 mg/L. Transcriptome analysis of *S. sclerotiorum* treated with **6g** by RNA sequencing indicated the down-regulation of succinate dehydrogenase gene SDHA and SDHB, and the inhibition of TCA-cycle.

Keyword: Succinate dehydrogenase inhibitor, Fungicide, Thiazole carboxamide, Molecular docking

Introduction

Succinate dehydrogenase (SDH), also known as succinate-ubiquinone reductase (SQR) or respiratory protein complex II, is involved in the tricarboxylic acid cycle and mitochondrial electron transport.[1] Its inhibitors mainly bind to the ubiquinone pocket of SDH and disrupt the mitochondrial respiration chain, thus leading to the pathogen death.[2-3] Succinate dehydrogenase inhibitors (SDHIs) have been commercialized since the earliest launching of carboxin as fungicide in 1966.[4] To date, 19 commercial SDHI fungicides belonging to diverse chemical types, such as oxathilin carboxamides (carboxin), benzamides (fluopyram), pyridine carboxamides (boscalid), thiazole carboxamides (thifluzamide), furan carboxamides (fenfuram), thiophene carboxamide (isofetamid) and pyrazole carboxamides (fluxapyroxad, pydiflumetofen) have been used for plant protection (Figure 1).[5] SDHI becomes the hotspot of the novel fungicide development due to its novel mode of action and broad-spectrum of activity.[6] However, with the frequent and extensive application of SDHI fungicides, many resistant fungi have been reported.[7-9] Therefore, it's of great benefit to discover novel SDH inhibitor with improved potency.

It's clear that the SDHI possesses a substituted five- or six-membered ring core, an amide bond and an amine moiety.[5] In terms of commercial SDHI, the most represented type contains the pyrazole, the substituents on the ring core are generally halogen, alkyl and haloalkyl, the current efforts mainly focus on the modification of

amine moiety.[10-13] Therefore, discovery of novel carboxyl core moiety would be another important direction with great chances for the novel SDHI development.

Different heterocycles always display different biological functions,[14,15] both the N and S containing heterocycles such as thiazole derivatives exhibit various biological activity,[16-18] for example, ethaboxam is a tubulin polymerization and oxidative respiration inhibitor used for oomycetes control,[19] thiazopyr inhibit cell division by disrupting spindle microtubule formation and is used as herbicide for pre-emergence annual grass and some broad-leaved weeds control,[20] while thiacloprid acts as an agonist of the nicotinic acetylcholine receptor in the insect central nervous system and is used by foliar application against sucking and biting insects.[21] Our group discovers different piperdinyl thiazole and isothiazole derivatives with different fungicidal activity and mode of actions.[22-24]

To continue our sustainable studies on five-membered heterocyclic based novel pesticide development with various novel lead structures and mode of action, here, homology modeling and structure-based molecular design strategies were used for novel SDHI development (Figure 2). We firstly built the three-dimensional (3D) protein models of SDH from *Sclerotinia sclerotiorum* using SWISS-MODEL. By molecular docking of fluxapyroxad with *S. sclerotiorum* SDH (SsSDH), 200 compounds with different five-membered heterocyclic carboxyl core moieties were designed according to the structure characteristics of reported SDHI, pesticide molecular design principles and experience. After docking these ligands into SsSDH,

six candidates were identified (Figure S1). 4-Hydroxy thiazole was identified as carboxyl core moiety according to the binding affinity energies and synthesis feasibility. Herein, a novel series of thiazole carboxamide derivatives containing hydroxy or alkoxy substituent at the 4-position of thiazole were designed and synthesized for biologically evaluation. Pesticide target discovery and target validation of the new lead compound were the same important tasks for novel pesticide development.[25] Docking and structure activity relationship (SAR) studies were further conducted to validate the key structural features responsible for their fungicidal potency. Transcriptome analysis of the highly active compound **6g** was also performed by RNA sequencing analysis for their target validation.

Materials and Methods

Equipment and materials: Melting points of new compounds were determined on an X-4 melting point apparatus. ^{1}H NMR (400 MHz) and ^{13}C NMR (101 MHz) spectra were taken on Bruker Avance 400 MHz spectrometer in $CDCl_3$ or DMSO-d_6 solution. High resolution mass spectra (HRMS) were obtained by using a 7.0 T FTICR-MS instrument. Crystal structure was recorded on a Bruker SMART 1000CCD diffraction meter.

Synthesis of Ethyl 4-Hydroxy-2-methyl Thiazole-5-carboxylate (2). Compound **2** was synthesized according to the revisions of previously reported procedures.[26] Pyridine (73.2 g, 0.78 mol) was added to a solution of compound **1** (20.0 g, 0.26 mol) in ethanol (250 mL). Diethyl 2-bromomalonate was then added

and the mixture was heated at 78°C for 2 h. After cooling of the mixture, the solvent was removed by rotary evaporation and the crude residue was dissolved in ethyl acetate (200 mL). The solution was washed with HCl (1 mol/L, 150 mL × 2) and saturated brine (100 mL), the organic layer was dried over anhydrous sodium sulfate, filtered and concentrated under reduced pressure. The residue was recrystallized from ethanol to give white crystal of compound **2** (39.0 g 78%), m.p.: 37-39°C; ^{1}H NMR (400 MHz, $CDCl_3$) δ 4.36 (q, J = 7.1 Hz, 2H, OCH_2), 2.67 (s, 3H, thiazole-CH_3), 1.37 (t, J = 7.1 Hz, 3H, OCH_2-$\underline{CH_3}$); ^{13}C NMR (101 MHz, $CDCl_3$) δ 170.25, 169.02, 165.71, 95.96, 61.52, 20.29, 14.31; HRMS (ESI) *m/z* calcd for $C_7H_{10}NO_3S$ $[M + H]^+$: 188.0376; found: 188.0374.

Synthesis of Ethyl 4-Alkoxy-2-methyl Thiazole-5-carboxylate (3). To a solution of compound **2** (11.0 g, 0.059 mol) in acetone (200 mL), CH_3I or alkyl bromide (0.118 mol) was added, followed by the addition of Ag_2O (14.98 g, 0.065 mol). The reaction mixture was stirred at room temperature for 8 h. The suspension was filtered and concentrated under reduced pressure. The residue was purified by silica gel column chromatography with petroleum ether (60-90°C fraction):EtOAc (30:1-20:1) as eluent to afford compounds **3.**

*Data for **3a***: yellow oil; yield, 75%; ^{1}H NMR (400 MHz, $CDCl_3$) δ 4.21 (q, J = 7.0 Hz, 2H, OCH_2), 4.05 (s, 3H, OCH_3), 2.55 (s, 3H, thiazole-CH_3), 1.25 (t, J = 7.0 Hz, 3H, OCH_2-$\underline{CH_3}$); ^{13}C NMR (101 MHz, $CDCl_3$) δ 167.66, 165.43, 161.38, 99.93,

60.64, 58.12, 20.08, 14.38; HRMS (ESI) *m/z* calcd for $C_8H_{12}NO_3S$ $[M + H]^+$: 202.0533; found: 202.0536.

*Data for **3b***: yellow oil; yield, 50%; ^{1}H NMR (400 MHz, $CDCl_3$) δ 5.01 (d, J = 2.4 Hz, 2H, C-CH_2), 4.21 (q, J = 7.1 Hz, 2H, OCH_2), 2.56 (s, 3H, thiazole-CH_3), 2.44 (t, J = 2.3 Hz, 1H, CH), 1.26 (t, J = 7.1 Hz, 3H, CH_2-$\underline{CH_3}$); ^{13}C NMR (101 MHz, $CDCl_3$) δ 167.73, 163.18, 161.00, 101.54, 78.52, 75.19, 60.76, 57.97, 20.09, 14.33; HRMS (ESI) m/z calcd for $C_{10}H_{12}NO_3S$ $[M + H]^+$: 226.0538; found: 226.0534.

Synthesis of Ethyl 4-Methoxy-2-methyl Thiazole-5-carboxylic Acid (4). Compound **2** was synthesized according to the revisions of previously reported procedures.[26] To a round bottom flask containing compound **3** (5.87 mg, 29.17 mmol) and KOH (30 mL of a 2 mol/L solution in methanol) was added. The solution was then heated at 65°C for 2h and the solvent was removed under reduced pressure. The residue was added water and acidified to about pH 2 with 2 mol/L HCl. The suspension was then filtered and filter cake was dried to obtain the compound **4** (4.09 g, 81%) as yellow powder, m.p.: 181-183°C; ^{1}H NMR (400 MHz, DMSO-d_6) δ 3.97 (s, 3H, OCH_3), 2.59 (s, 3H, thiazole-CH_3); ^{13}C NMR (101 MHz, DMSO-d_6) δ 167.97, 164.03, 161.86, 100.23, 57.65, 19.73; HRMS (ESI) *m/z* calcd for $C_6H_8NO_3S$ $[M + H]^+$: 174.0220; found: 174.0220.

General Synthesis Procedures of the Compounds 5a-5q. To a solution of compounds **4** (0.2 g, 1.15 mmol) in DMF (4 mL), N,N-diisopropylethylamine (DIPEA, 0.57 mL, 3.45 mmol) and (3-hydroxy-3H-1,2,3-thiazolo[4,5-b]pyridinato-O)

tri-1-pyrrolidinylphosphonium hexafluorophosphate (PyAOP, 0.66 g, 1.27 mmol) were added at 0°C. The mixture was stirred at 0°C for 15 mins and the corresponding amine (1.04 mmol) was added. The reaction was warmed to room temperature or 75°C according to the corresponding amine and stirred until TLC analysis showed complete consumption of amine. The reaction mixture was dissolved in water (50 mL) and extracted with dichloromethane (25 mL × 3). The combined organic layer was washed with saturated brine (50 mL), dried over anhydrous sodium sulfate, filtered and concentrated under educed pressure. The residue was purified by silica gel column chromatography with petroleum ether (60-90°C fraction):EtOAc (35:1-2:1) as eluent to afford the title compounds **5a-5r** (25-98%).

General Synthesis Procedures of the Compounds 6a-6n. The compound **5a-5q** (0.60 mmol) was dissolved in dry dichloromethane (10 mL) and cooled to -20°C. The solution of BCl_3 in dichloromethane (1 mol/L, 2 mL, 2.0 mmol) was dropwised and the mixture was stirred for 0.5-3 h. The reaction was quenched by the addition of aqueous saturated $NaHCO_3$ (10 mL) and extracted with dichloromethane (10 mL × 3). The combined organic layer was washed with saturated brine (20 mL), dried over anhydrous sodium sulfate, filtered and concentrated under reduced pressure. The residue was recrystallized from methanol to give the title compounds **6a-6n** (32-99%).

Single Crystal X-ray Diffraction Data Collection

Single crystal X-ray diffraction data of compounds **5l** and **6d** were collected on a Rigaku Saturn 724 CCD system using Mo Kα radiation. Unique reflections with R_{int} and $I > 2\sigma(I)$ were collected for refinements. The structure was directly solved by SHELXS-97 program and hydrogens were introduced in idealized positions according to the theoretical models. The derived atomic parameters were refined through full matrix least-squares.

Fungicidal Activities

The fungicidal activities of synthesized compounds against *A. s: Alternaria solani; B. c: Botrytis cinerea; C. a: Cercospora arachidicola; G. z: Gibberella zeae; P. i: Phytophthora infestans (Mont) de Bary; P. p: Physalospora piricola; P. s: Pellicularia sasakii; R. c: Rhizoctonia cerealis; S. s: Sclerotinia sclerotiorum* were evaluated *in vitro* at 50 mg/L for the preliminary screening according to the previously reported procedures.[27] The commercial SDHI fungicide thifluzamide was selected as positive control. Compounds with good inhibitory activities were further evaluated for their median effective concentration (EC_{50}) values detection by the established procedures.[27] All experiments were tested and repeated for three times. Data were presented as the mean ± standard deviation.

The *in vivo* fungicidal activity of the target compounds against *S sclerotiorum* was carried out on *Brassica napus* L. leaves. For protective activity assay, healthy leaves of *Brassica napus* L. were sprayed with target the compounds (2.0 mg/L) respectively and then cultivated at 25°C for 24 h before inoculation with *S*

sclerotiorum. For curative activity assay, healthy leaves of *B. napus* L. were sprayed with the target compounds (2.0 mg/L) respectively and then cultivated at 25°C for 24 h after inoculation with *S sclerotiorum*. For inactivation activity assay, *S sclerotiorum* treated with the target compounds (2.0 mg/L) respectively and then cultivated at 25°C for 0.5 h before inoculation. The results were observed as diameters of the lesion after cultivation at 25°C for 36 h. Thifluzamide (5.0, 10.0 mg/L) was chosen as the positive control. The disease control efficacy (%) was calculated as (c - d) / (c - 0.5) × 100, where c is the diameter (cm) of the blank, and d is the diameter (cm) of the treatment. Each treatment was performed for three times.

SDH Enzymatic Inhibition Activities

The SDH enzymatic activity was determined using the succinate dehydrogenase assay kit (Solarbio, BC0950). *S. sclerotiorum* grew in Fries medium for 5 days and then treated with various concentrations of the chosen active compounds. The SDH enzymatic activity was determined after treatment with compounds for 24 h and the absorbance at 600 nm was obtained by a microplate reader. Compounds were tested at 6 different concentrations at 0.05 - 20 mg/L and each compound was repeated for three times. The IC_{50} values were calculated by GraphPad Prim version 6.02.

The Modeling and Molecular Docking Analysis

The 3D structure profile of SsSDH (A Subunit, SS1G_07864; B Subunit, SS1G_04384; C Subunit, SS1G_01661; D Subunit, SS1G06173) were modelled using SWISS-MODEL with default parameters. Protein structure of individual subunits

were built by YASARA and evaluated by Ramachandran plot, then precise structures of the subunits were align to *Ss*SDH structure profile which modeled by SWISS-MODEL in order to form the accurate final structure. And the ligand binding center of *Ss*SDH was identified by Autodock Tools[28-29] with carboxin, the ligand of succinate dehydrogenase. The structures of ligands were optimized with the ligand minimization protocol. The molecular docking analysis was performed by the Autodock Tools with default values. The structure of complexes which analyzed by docking were showed by Ligplot.[30]

RNA Sequencing and Data Analysis

S. sclerotiorum was grown in PDA at 25°C for 1 week, and subsequently treated with compound **6g** at 0.1 mg/L for 36 hours, with DMF used as control. Total RNA of samples was extracted using TRIzol Reagent (Invitrogen, USA). cDNA libraries were constructed using a Truseq stranded mRNA kit (Illumina, San Diego, USA). Sequencing was conducted on an Illumina MiSeq sequencing system using the HiSeq 4000 SBS Kit (Illumina, San Diego, USA) following the manufacturer's instructions and *S. sclerotiorum* genome database was used as a reference for mapping the short reads. The count data were normalized to generate effective library using Trimmed Means of Means (TMM) values. Statistical analysis was performed with these data using a generalized linear model linked to the negative binomial distribution performed using the EdgeR package. The different expression genes were identified

with FDR ≤ 0.05 and fold change ＞ 1.5 (or fold change < 0.67). The Kyoto Encyclopedia of Genes and Genomes (KEGG) pathway for each gene were extracted.

Results and Discussion

Chemical Synthesis

The synthetic route for the compounds **5a-5r** and **6a-6n** was described in Figure 3. Thioamide **1** was reacted with diethyl 2-bromomalonate to yield the 4-hydroxythiazole **2**, which underwent silver oxide mediated methylation to provide ether **3**. Hydrolysis of intermediate **3** in the solution of potassium hydroxide in methanol obtained acid **4**, which was coupled with various amines to give the corresponding amides **5a-5r** in the yield of 25-98%. The compounds **6a-6n** were obtained by demethylation of compounds **5a-5q** in a yield of 38-99%**.** The chemical structures of all the title compounds **5a-5r** and **6a-6n** were confirmed by ^{1}H NMR, ^{13}C NMR and HRMS, All the physical and chemical properties of the target compounds were shown in the supporting information.

The molecule structure of the target compounds **5l** (CCDC: 1877458) and **6d** (CCDC: 1877459) were further identified by single crystal X-ray analysis as shown in Figure 4 and Table S1. Both the X-ray detected structures of **5l** and **6d** were accorded with its theoretical molecular structures.

Fungicidal Activities and SAR Discussion

To evaluate the fungicidal activities of all the target compounds, the *in vitro* fungicidal activity determination against nine representative plant pathogens, *A.*

solani, *B. cinerea*, *C. arachidicola*, *G. zeae, P. infestans*, *P. piricola*, *P. sasakii, R. cerealis* and *S. sclerotiorum,* were initially carried out at the concentration of 50 mg/L. As shown in Table 1, the target compounds **5i**, **5o**, **5p** and **5q** exhibited > 50% activity against 5-7 different kinds of fungi, and the results indicated that derivatives with a flexible amine such as benzylamine (**5o**), pyridylmethylamine (**5p**) and phenylethanamine (**5q**) had a broader fungicidal spectrum. On the contrary, the target compounds with more rigid amines, naphthylamine (**5k**) and tetrahydronaphthyl amine (**5l**) displayed very weak fungicidal activities against nine fungi tested. In addition, most of the compounds displayed promising fungicidal activities against *S. sclerotiorum, B. cinerea* and *R. cerealis* at 50 mg/L. Compound **5j** exhibited > 90% activity against the above three fungi, compounds **5i**, **5n**, **6a**, **6c**, **6d**, **6f**, **6g** and **6i** exhibited > 90% activity against both *S. sclerotiorum* and *R. cerealis.* Compounds **5a**, **5b**, **5c**, **5d**, **5f**, **5g**, **5q**, **6b**, **6e**, **6j**, **6k**, **6m** and **6n** exhibited > 90% activity against *S. sclerotiorum,* whereas compounds **5m** and **5p** exhibited > 90% activity against *B. cinerea*.

To further determine the fungicidal potency and probe the SAR of these novel thiazole carboxamide derivatives, their EC_{50} values were tested against *B. cinerea, R. cerealis* and *S. sclerotiorum,* the results were shown in Table 2. In general, compounds bearing a hydroxyl group at 4-position of thiazole showed better fungicidal activities than their corresponding alkoxyl-substituted analogues. For example, **6c** (EC_{50} = 13.2, 1.3 mg/L) was more active than **5c** (EC_{50} = 108.5, 20

mg/L); **6d** (EC_{50} = 4.7, 9.8 mg/L) was more active than **5f** (EC_{50} = 59.4, 17.0 mg/L); **6f** (EC_{50} = 1.2, 2.3 mg/L) was more active than **5h** (EC_{50} > 100 mg/L, > 100 mg/L); **6l** (EC_{50} = 40.3, 4.8 mg/L) was more active than **5o** (EC_{50} > 100 mg/L, = 23.4 mg/L) against *R. cerealis* and *S. sclerotiorum*, respectively. Compound **5i** (with 3,4-F_2-phenyl group at the ortho-position of aniline) showed better fungicidal activity than **5h** (with 3,4,5-F_3-phenyl group at the same position), which indicated that the 3,4-F_2-phenyl group at the ortho-position of aniline was more favorable for the hydrophobic interactions with SDH. As for hydroxyl-substituted thiazole series **6**, we initially explored the effect of substituents on aniline moiety, especially substituents at the ortho-positions. The results indicated that introduction of bulky alkyl groups (**6c**) and halophenyl groups (**6d**, **6f** and **6g**) at the ortho-position of aniline were favorable for the fungicidal activities against *S. sclerotiorum* and *R. cerealis,* but not all the fungi showed this rule. Among them, **6f** (EC_{50} = 1.2, 2.3 and 33.7 mg/L) and **6g (**EC_{50} = 6.2, 0.6 and 42.3 mg/L) displayed the most potent fungicidal activities against *R. cerealis*, *S. sclerotiorum* and *B. cinerea,* respectively. In addition, substituting the aniline moiety with other amines, including flexible alkyl amines, naphthyl amine and cyclic amines, was also studied. The results indicated that, naphthylamine (**5k**) and tetrahydronaphthyl amine (**5l**) substituents decreased the fungicidal activities of the target compounds.

Among these novel derivatives, compounds **5i**, **5j**, **5n**, **6a**, **6c**, **6d**, **6f**, **6g** and **6i** displayed improved fungicidal activities with EC_{50} of 1.2 - 16.4 mg/L against *R.*

cerealis as compared to thifluzamide with EC_{50} of 22.1 mg/L. Surprisingly, compound **6f** showed the highest fungicidal activity against *R. cerealis* with an EC_{50} value of 1.2 mg/L, which was about 18-times more active than that of the thifluzamide. As for *S. sclerotiorum,* compounds **5a**, **6b**, **6c**, **6f**, **6i**, **6g** and **6k** exhibited improved fungicidal activities with EC_{50} of 0.5 - 1.9 mg/L as compared to the thifluzamide with EC_{50} of 4.4 mg/L. In particular, compound **5a** with EC_{50} of 0.5 mg/L and compound **6g** with EC_{50} of 0.6 mg/L displayed 7 - 9 times higher inhibitory activity than thifluzamide against *S. sclerotiorum*. While, compounds **5j**, **5m**, **5o** and **6n** showed comparable activity with EC_{50} of 11.3 - 13.1 mg/L as compared to the thifluzamide with EC_{50} of 10.4 mg/L against *B. cinerea*.

***In Vivo* Fungicidal Activities**

According to the results of the *in vitro* fungicidal assay, compounds **5i**, **6c**, **6f** and **6g** were chosen and further evaluated their greenhouse fungicidal activity *in vivo* for controlling the *S. sclerotiorum* in *B. napus* L. As shown in Figure 5, compounds **6c** and **6g** showed promising protective activity of 75.4% and 67.3% (Table 3) respectively at a concentration of 2.0 mg/L, while compounds **5i** (2.0 mg/L), **6f** (2.0 mg/L) and the positive control thifluzamide (10.0 mg/L) with negligible protective activity. In curative activity assay, tested compounds **5i**, **6c**, **6f** and **6g** displayed improved efficacy of 17.1 – 56.7% at the concentration of 2.0 mg/L than thifluzamide (5.0 mg/L) with curative activity of 14.9%. In inactivation activity assay, compounds **6c** and **6g** showed promising protective activity of 83.9% and 86.1% respectively at

289 the concentration of 2.0 mg/L, which were similar to that of thifluzamide with
290 inactivation activity of 92.5% at the concentration of 5.0 mg/L. The results further
291 indicated that, compounds **6c** and **6g** had great potential for the novel fungicide
292 development.

293 **SDH Enzymatic Inhibition Activities**

294 Target discovery and identification is an essential basis for novel pesticide
295 development and success opportunity improvement.[25, 31] Enzymatic bioassay of
296 compounds **5i**, **5j**, **6c**, **6f** and **6g** with promising fungicidal activities were selected and
297 further evaluated for SDH enzymatic inhibition. As showed in Table 4, compounds **5i**,
298 **5j**, **6c**, **6f** and **6g** displayed SDH inhibitory activities with IC_{50} values of 2.27, 10.77,
299 0.89, 2.28 and 0.56 mg/L respectively, this trend was very similar to the results of
300 their fungicidal activity against *S. sclerotiorum* bioassay. Compound **6g** exhibited the
301 best inhibitory activity with IC_{50} value of 0.56 mg/L at the same level of the
302 thifluzamide with IC_{50} of 0.55 mg/L.

303 **Docking Analysis**

304 In order to elucidate the possible mechanism of newly synthesized thiazole
305 carboxamide derivatives and further explain the SAR, the 3D structure of *Ss*SDH was
306 modeled and the docking analysis was performed. Ramachandran plot showed that the
307 structure of *Ss*SDH was a good quality of model (Figure S2), which had a better
308 overlap with template proteins (2WQY, Figure S3). All of the derivatives were
309 docked into the active site of *Ss*SDH and the docking scores were shown in Table S3.

The detailed interactions of two representative derivatives (**6g** and **5l**) with *Ss*SDH were provided in Figure 6. Active compound **6g** (Figure 6A) showed the similar binding mode with that of commercial fluxapyroxad (Figure 2). The amide group of **6g** and fluxapyroxad formed a hydrogen bond with the side chain of Trp230. Moreover, the halophenyl moiety at the ortho-position of aniline was deeply buried into the active site by hydrophobic interactions. While all the favorable interactions were absent from the docked complex of inactive compound **5l** and *Ss*SDH (shown in Figure 6B), which resulted in the sharply decreased fungicidal activity of **5l**. In order to confirm the accuracy of the molecular docking, combining the homology analysis results of *Ss*SDH and 2WQY (data not shown) with the single crystal data of 2WQY. Trp172， Trp173, Trp32 and Pro169 were identified as the binding site between carboxin and protein, Arg43 was the binding site of Heme. It was consistent with the docking results, the same binding site in *Ss*SDH were Trp229, Trp230, Trp81, Pro146 and Arg88, which were **6g** and Heme binding site respectively (Figure 6A).

The RNA-seq Analysis of *S. sclerotiorum* Treated with 6g

The different expression genes (DGEs) affected by **6g** was identified by RNA sequencing. Totally 2831 DGEs with fold changes > 1.5 (or < 0.67) were identified in **6g** vs CK. Among these DGEs, there were 1562 up-regulated genes and 1269 down-regulated genes. As indicated in Figure 7, the expression of succinate dehydrogenase gene SDHA and SDHB were down-regulated. Because of the activity down-regulation of the SDH, the whole TCA-cycle in fungi was inhibited, and thus

led to the down-regulation of aconitase (ACO1 and ACO2), isocitrate dehydrogenase (IDH1, IDH2 and IDH3), 2-oxoglutarate dehydrogenase (OGDH1), succinate-CoA ligase (LSC1), fumarate hydratase (FUMC), and malate dehydrogenase (MDH2). While, the pathway for citric acid formation by oxaloacetate in TCA cycle was inhibited, and thus resulting in significant up-regulation of the phosphoenolpyruvate carboxykinase (PCK1) which converted oxaloacetate into phosphoenolpyruvate and carbon dioxide, and the down–regulation of the pyruvate carboxylase (PYC1) which converted pyruvate into oxaloacetate. However, the expression of pyruvate kinase (PK) and citrate synthase (CS) were not significantly changed.

To further identify the function of the biological pathways in *S. sclerotiorum* which affected by **6g**, the KEGG pathway was performed for functional enrichment classification of the 2381 DGEs. As shown in Figure 8, the biological process in the pentose and the glucuronate interconversion, starch and sucrose metabolism, and TCA cycle had a significant enrichment change. Additionally, the pyruvate metabolism, fatty acid degradation, and amino acid metabolism were also changed, which was reported to be related to TCA cycle.[32]

Abbreviations Used

SDH, succinate dehydrogenase; EC_{50}, median effective concentration; DIPEA, N,N-diisopropylethylamine; PyAOP, (3-hydroxy-3H-1,2,3-thiazolo[4,5-*b*]pyridinato -O)tri-1-pyrrolidinylphosphonium hexafluorophosphate; TMM, Trimmed Means of

Means values; KEGG. Kyoto Encyclopedia of Genes and Genomes; DGEs, different expression genes; IDH, isocitrate dehydrogenase; OGDH1, 2-oxoglutarate dehydrogenase; LSC, succinate-CoA ligase; FUMC, fumarate hydratase; MDH, malate dehydrogenase; PCK, phosphoenolpyruvate carboxykinase; PYC, pyruvate carboxylase; PK, pyruvate kinase; CS, citrate synthase.

Acknowledgment

This work was supported in part by the National Natural Science Foundation of China (No. 31571991, No. 31872007 and No. 3181101739), the Tianjin Natural Science Foundation (No. 18JCZDJC33500), the China Postdoctoral Science Foundation (No. 2017M611156), and the International Science & Technology Cooperation Program of China (No. 2014DFR41030). We gratefully thank Huabao Chen in College of Agronomy, Sichuan Agricultural University for the *in vivo* experiments of the compounds against *S. sclerotiorum* on *Brassica napus* L. leaves.

Supporting Information

^{1}H NMR, ^{13}C NMR data for the target compounds; Crystal data of **5l** and **6d**; EC_{50} value of target compounds. This material is available free of charge via the Internet at http: //pubs.acs.org.

References

(1) Oyedotun, K. S.; Lemire, B. D. The quaternary structure of the *Saccharomyces*

373 *cerevisiae* succinate dehydrogenase. Homology modeling, cofactor docking, and
374 molecular dynamics simulation studies. *J. Biol. Chem.* **2004**, *279*, 9424-9431.
375 (2) Sun, F.; Huo, X.; Zhai, Y.; Wang, A.; Xu, J.; Su, D.; Bartlam, M.; Rao, Z. Crystal
376 structure of mitochondrial respiratory membrane protein complex II. *Cell* **2005**, *121*,
377 1043-1057.
378 (3) Horsefield, R.; Yankovskaya, V.; Sexton, G.; Whittingham, W.; Shiomi, K.;
379 Omura, S.; Byrne, B.; Cecchini, G.; Iwata, S. Structural and computational analysis of
380 the quinone-binding site of complex II (succinate-ubiquinone oxidoreductase): a
381 mechanism of electron transfer and proton conduction during ubiquinone reduction. *J.*
382 *Biol. Chem.* **2006**, *281*, 7309-7316.
383 (4) DellaGreca, M.; Iesce, M. R.; Cermola, F.; Rubino, M.; Isidori, M.
384 Phototransformation of carboxin in water. Toxicity of the pesticide and its sulfoxide
385 to aquatic organisms. *J. Agric. Food Chem.***2004**, *52*, 6228-6232.
386 (5) Sierotzki, H.; Scalliet, G. A review of current knowledge of resistance aspects for
387 the next-generation succinate dehydrogenase inhibitor fungicides. *Phytopathol.* **2013**,
388 *103*, 880-887.
389 (6) Keohane, C. E.; Steele, A. D.; Fetzer, C.; Khowsathit, J.; Van Tyne, D.; Moynie,
390 L.; Gilmore, M. S.; Karanicolas, J.; Sieber, S. A.; Wuest, W. M. Promysalin elicits
391 species-selective inhibition of *Pseudomonas aeruginosa* by targeting succinate
392 dehydrogenase. *J. Am. Chem. Soc.* **2018**, *140*, 1774-1782.
393 (7) De Miccolis Angelini, R. M.; Masiello, M.; Rotolo, C.; Pollastro, S.; Faretra, F.

394 Molecular characterisation and detection of resistance to succinate dehydrogenase
395 inhibitor fungicides in *Botryotinia fuckeliana* (*Botrytis cinerea*). *Pest Manag. Sci.*
396 **2014**, *70*, 1884-1893.
397 (8) Avenot, H. F.; Sellam, A.; Karaoglanidis, G.; Michailides, T. J. Characterization
398 of mutations in the iron-sulphur subunit of succinate dehydrogenase correlating with
399 Boscalid resistance in *Alternaria alternata* from *California pistachio*. *Phytopathol.*
400 **2008**, *98*, 736-742.
401 (9) Rehfus, A.; Strobel, D.; Bryson, R.; Stammler, G. Mutations in sdh genes in field
402 isolates of *Zymoseptoria tritici* and impact on the sensitivity to various succinate
403 dehydrogenase inhibitors. *Plant Pathol.* **2018**, *67*, 175-180.
404 (10) Xiong, L.; Li, H.; Jiang, L. N.; Ge, J. M.; Yang, W. C.; Zhu, X. L.; Yang, G. F.
405 Structure-based discovery of potential fungicides as succinate ubiquinone
406 oxidoreductase inhibitors. *J. Agric. Food Chem.* **2017**, *65*, 1021-1029.
407 (11) Wen, F.; Jin, H.; Tao, K.; Hou, T. Design, synthesis and antifungal activity of
408 novel furancarboxamide derivatives. *Eur. J. Med. Chem.* **2016**, *120*, 244-251.
409 (12) Li, S.; Li, D.; Xiao, T.; Zhang, S.; Song, Z.; Ma, H. Design, Synthesis, fungicidal
410 activity and unexpected docking model of the first chiral boscalid analogues
411 containing oxazolines. *J. Agric. Food Chem.* **2016**, *64*, 8927-8934.
412 (13) Zhang, A.; Zhou, J.; Tao, K.; Hou, T.; Jin, H. Design, synthesis and antifungal
413 evaluation of novel pyrazole carboxamides with diarylamines scaffold as potent
414 succinate dehydrogenase inhibitors. *Bioorg. & Medic. Chem. Let.* **2018**, *28*,

3042-3045.

(14) Zhang, L.; Li, W.; Xiao, T.; Song, Z.; Csuk, R.; Li, S. Design and discovery of novel chiral antifungal amides with 2-(2-oxazolinyl)aniline as a promising pharmacophore. *J. Agric. Food Chem.* **2018**, *66*, 8957-8965.

(15) Obydennov, K. L.; Khamidullina, L. A.; Galushchinskiy, A. N.; Shatunova, S. A.; Kosterina, M. F.; Kalinina, T. A.; Fan, Z.; Glukhareva, T. V.; Morzherin, Y. Y. Discovery of methyl (5Z)-[2-(2,4,5-trioxopyrrolidin-3-ylidene)-4-oxo-1,3-thiazolidin-5-ylidene]acetates as antifungal agents against potato diseases. *J. Agric. Food Chem.* **2018**, *66*, 6239-6245.

(16) Liu, A.; Wang, X.; Liu, X.; Li, J.; Chen, H.; Hu, L.; Yu, W.; He, L.; Liu, W.; Huang, M. Synthesis and fungicidal activity of novel 2‐heteroatomthiazole‐based carboxanilides. *J. Heterocycl. Chem.* **2017**, *54*, 1625-1629.

(17) Xue, H.; Liu, A.; Liu, W.; Li, J.; Ren, Y.; Huang, L.; He, L.; Ou, X.; Ye, J.; Huang, M. Syntheses and fungicidal activities of thiazole-5-carboxanilides bearing thioether group. *Chem. Res. Chin. Univ.* **2016**, *32*, 781-785.

(18) Kumar, S.; Ranjana A. Thiazole: a privileged motif in marine natural products. *Mini-Rev. Org. Chem.* **2019**, *16*, 26-34.

(19) Kim, D. S.; Chun, S. J.; Jeon, J. J.; Lee, S. W.; Joe, G. H. Synthesis and fungicidal activity of ethaboxam against Oomycetes. *Pest Manag. Sci.* **2004**, *60*, 1007-1012.

(20) Reade, J. P.; Cobb, A. Herbicides: modes of action and metabolism. In *Weed*

436 *Management Handbook*, 9; Robert, E. L.; Wiley-Blackwell: 2002; 9, 134-157.

437 (21) Zhang, H. J.; Zhou, Q. W.; Zhou, G. C.; Cao, Y. M.; Dai, Y. J.; Ji, W. W.; Shang,

438 G. D.; Yuan, S. Biotransformation of the neonicotinoid insecticide thiacloprid by the

439 bacterium Variovorax boronicumulans strain J1 and mediation of the major metabolic

440 pathway by nitrile hydratase. *J. Agric. Food Chem.* **2011**, *60*, 153-159.

441 (22) Chen, L.; Zhu, Y. J.; Fan, Z. J.; Guo, X. F.; Zhang, Z. M.; Xu, J. H.; Song, Y. Q.;

442 Yurievich, M. Y.; Belskaya, N. P.; Bakulev, V. A. Synthesis of 1, 2, 3-thiadiazole and

443 thiazole-based strobilurins as potent fungicide candidates. *J. Agric. Food Chem.* **2017**,

444 *65*, 745-751.

445 (23) Chen, L.; Zhao, B.; Fan, Z.; Liu, X.; Wu, Q.; Li, H.; Wang, H. Synthesis of novel

446 3, 4-chloroisothiazole-based imidazoles as fungicides and evaluation of their mode of

447 action. *J. Agric. Food Chem.* **2018**, *66*, 7319-7327.

448 (24) Wu, Q. F.; Zhao, B.; Fan, Z. J.; Zhao, J. B.; Guo, X. F.; Yang, D. Y.; Zhang, N.

449 L.; Yu, B.; Kalinina, T.; Glukhareva, T. Design, synthesis and fungicidal activity of

450 isothiazole–thiazole derivatives. *RSC Adv.* **2018**, *8*, 39593-39601.

451 (25) Zhao, B.; Fan, S.; Fan, Z.; Wang, H.; Zhang, N.; Guo, X.; Yang, D.; Wu, Q.; Yu,

452 B.; Zhou, S. Discovery of pyruvate kinase as a novel target of new fungicide

453 candidate 3-(4-Methyl-1,2,3-thiadiazolyl)-6-trichloromethyl-[1,2,4]-triazolo-[3,4-b]

454 [1,3,4]-thiadizole. *J. Agric. Food Chem.* **2018**, *66*, 12439-12452.

455 (26) Goldberg, F. W.; Dossetter, A. G.; Scott, J. S.; Robb, G. R.; Boyd, S.;

456 Groombridge, S. D.; Kemmitt, P. D.; Sjogren, T.; Gutierrez, P. M.; deSchoolmeester,

457 J.; Swales, J. G.; Turnbull, A. V.; Wild, M. J. Optimization of brain penetrant
458 11beta-hydroxysteroid dehydrogenase type I inhibitors and in vivo testing in
459 diet-induced obese mice. *J. Med. Chem.* **2014**, *57*, 970-986.
460 (27) Fan, Z.; Yang, Z.; Zhang, H.; Mi, N.; Wang, H.; Cai, F.; Zuo, X.; Zheng, Q.;
461 Song, H. Synthesis, crystal structure, and biological activity of 4-methyl-1,2,3-
462 thiadiazole-containing 1,2,4-triazolo[3,4-b][1,3,4]thiadiazoles. *J. Agric. Food Chem.*
463 **2010**, *58*, 2630-2636.
464 (28) Di Muzio, E.; Toti, D.; Polticelli, F. DockingApp: a user friendly interface for
465 facilitated docking simulations with AutoDock Vina. *J. Comput. Aided Mol. Des.*
466 **2017**, *31*, 213-218.
467 (29) Morris, G. M.; Goodsell, D. S.; Huey, R.; Olson, A. J. Distributed automated
468 docking of flexible ligands to proteins: parallel applications of AutoDock 2.4. *J.*
469 *Comput. Aided Mol. Des.* **1996**, *10*, 293-304.
470 (30) Laskowski, R. A.; Swindells, M. B. LigPlot+: multiple ligand-protein interaction
471 diagrams for drug discovery. *J. Chem. Inf. Model.* **2011**, *51*, 2778-2786.
472 (31) Zhu, Y. J.; Wu, Q. F.; Fan, Z. J.; Huo, J. Q.; Zhang, J. L.; Chen, L.; Qian, X. L.;
473 Ma, D. J.; Wang, D. W. Synthesis, bioactivity and mode of action of $5_A5_B6_C$ tricyclic
474 spirolactones as novel antiviral lead compounds. *Pest Manag. Sci.* **2019**, *75*, 292-301.
475 (32) Yang, C.; Ko, B.; Hensley, C. T.; Jiang, L.; Wasti, A. T.; Kim, J.; Sudderth, J.;
476 Calvaruso, M. A.; Lumata, L.; Mitsche, M.; Rutter, J.; Merritt, M. E.; DeBerardinis,
477 R. J. Glutamine oxidation maintains the TCA cycle and cell survival during impaired

478 mitochondrial pyruvate transport. *Mol. Cell* **2014**, *56*, 414-424.

FIGURE CAPTIONS

Figure 1. Representative chemical structure of commercialized succinate dehydrogenase inhibitor (SDHI) fungicides.

Figure 2. Molecular design of the target compounds.

Figure 3. General synthetic procedure for the target compounds **5a-5r** and **6a-6n**. Reagents and conditions: (i) diethyl 2-bromomalonate, pyridine, ethanol, 78^{o}C, 5 h; (ii) CH_3I or R^1Br, Ag_2O, acetone, r.t. 10 h; (iii) 2 mol/L KOH in MeOH, 2 mol/L HCl, 65^{o}C, 2 h; (iv) DIPEA, PyAOP, amine, DMF, r.t. 10 h; (v) 2 mol/L BCl_3 in CH_2Cl_2, CH_2Cl_2, -20^{o}C, 2 h.

Figure 4. X-ray crystal structure of compounds **5l** (A) and **6d** (B).

Figure 5. *In vivo* activity of target compounds against *S. sclerotiorum* infected cole leaves. (A) Protective activity. (B) Curative activity. (C) Inactivation activity.

Figure 6. Binding modes of **6g** (A) and **5l** (B) with *S. sclerotiorum* SDH.

Figure 7. The expression of metabolic enzyme related genes in TCA cycle in *S. sclerotiorum* treated with **6g**. Citrate synthase, CS1 (SS1G_04899). Aconitase, ACO1 (SS1G_11047), ACO2 (SS1G_10635). Isocitrate dehydrogenase, IDH1 (SS1G_04924), IDH2 (SS1G_09958), IDH3 (SS1G_04160). 2-Oxoglutarate dehydrogenase, OGDH1 (SS1G_05934). Succinate-CoA ligase, LSC1 (SS1G_07524). Succinate dehydrogenase, SDH1 (SS1G_07864), SDH2 (SS1G_04384). Fumarate hydratase, FUMC (SS1G_05243). Malate dehydrogenase, MDH2 (SS1G_13825).

499 Phosphoenolpyruvate carboxykinase, PCK1 (SS1G_02281). Pyruvate carboxylase,

500 PYC1 (SS1G_12839). Pyruvate kinase, PK (SS1G_04568).

501 **Figure 8**. The DEGs enriched in the biological pathway.

Table 1. *In Vitro* Fungicidal Activities (Inhibition Rate[a] / %) of the Target Compounds at 50 mg/L

Compd	*A.s*[b]	*B.c*	*C.a*	*G.z*	*P.i*	*P.p*	*P.s*	*R.c*	*S.s*
5a	20.6±0.8	55.8±2.8	9.8±2.2	2.9±0.7	18.2±2.1	10.5±4.5	0	8.2±1.7	95.4±1.5
5b	14.7±1.1	27.8±1.0	5.9±1.5	8.8±1.5	36.4±2.2	13.2±4.8	0	48.2±0.2	91.8±0.5
5c	29.4±4.2	86.7±0.2	13.7±4.9	26.5±4.7	18.2±2.4	13.2±4.5	7.3±3.6	50.6±1.1	90.1±3.3
5d	17.6±4.8	51.1±4.7	13.7±1.9	5.9±4.7	18.2±0.7	13.2±2.4	0	47.4±1.7	91.3±3.4
5e	38.2±0.1	69.4±1.1	37.3±4.9	11.8±3.7	22.7±2.1	26.3±4.1	7.3±2.0	51.0±1.2	82.9±0.2
5f	0	73.8±3.6	10.6±4.9	10.1±0.3	11.5±0.7	11.5±0.1	10.3±1.0	46.0±4.2	90.7±2.1
5g	10.0±4.5	41.7±2.1	15.7±4.5	10.5±3.5	18.0±0.5	12.5±3.9	11.3±4.7	80.2±2.9	95.7±1.8
5h	5.3±2.1	31.3±0.2	15.4±4.2	5.4±2.3	7.7±4.0	0	10.3±2.6	12.2±4.2	53.8±3.0
5i	67.6±1.1	50.0±4.0	88.2±3.9	58.8±0.6	22.7±0.1	5.3±2.1	12.2±2.2	96.9±0.8	95.0±2.9
5j	20.6±2.4	92.0±3.4	3.9±2.7	23.5±4.0	11.4±5.0	0	0	95.2±0.8	91.6±2.3
5k	29.4±2.2	41.7±2.2	21.6±3.8	17.6±5.8	13.6±1.2	26.3±1.9	12.2±2.7	38.2±4.9	46.4±2.2
5l	29.4±0.3	11.1±4.4	25.5±4.9	23.5±5.1	11.4±0.1	13.2±2	0	51.6±1.9	0
5m	23.5±3.2	90.0±2.1	29.4±1.6	0	18.2±4.4	0	0	85.1±0.7	80.8±4.0
5n	0.0±0.7	81.5±1.2	6.7±3.4	5.0±2.2	0	18.0±1.2	3.4±3.0	90.1±1.5	91.5±3.3
5o	52.9±4.5	41.7±0.6	54.9±4.3	54.2±4.3	18.2±4.9	26.3±1.2	12.2±2.6	81.0±1.1	83.6±3.2
5p	47.1±2.9	92.0±1.0	39.2±5.1	67.6±3.6	27.3±2.4	52.6±4.8	12.2±2.5	57.4±1.1	86.4±4.5
5q	88.2±2.0	69.4±3.0	68.6±3.1	70.6±0.5	54.5±0.3	46.1±1.7	36.6±0.6	70.7±3.9	90.9±1.0
5r	0	22.2±2.8	80.8±0.4	25.0±3.8	23.8±2.5	5.8±3.6	20.0±5.4	93.5±0.3	64.0±1.4
6a	23.5±4.5	47.5±1.6	13.7±2.4	5.9±4.1	20.5±4.6	26.3±4.4	0	94.3±3.2	93.1±0.8
6b	10.5±3.9	68.3±0.8	13.3±4.2	5.0±8.5	7.7±1.0	4.9±2.5	6.9±4.9	78.8±4.6	98.3±0.9
6c	23.5±1.7	55.6±3.0	5.9±3.8	8.8±4.6	27.3±1.4	44.7±3	0	90.7±2.0	95.6±3.7

6d	15.8±4.5	60.6±0.2	26.7±1.3	15.0±1.3	38.5±1.4	14.8±2.7	17.2±3.6	95.2±1.0	90.4±3.9
6e	21.1±0.7	60.0±2.2	33.5±3.5	5.3±3.1	0	18.0±3.4	27.6±2.8	36.6±3.6	91.6±2.3
6f	15.8±3.7	65.0±4.0	26.7±3.8	0	19.2±3.8	8.2±8.0	10.3±0.5	98.0±1.9	95.7±3.5
6g	47.1±0.8	60.0±3.5	19.6±4.3	23.5±4.0	31.8±1.6	39.5±3.1	12.2±0.2	91.0±3.6	100.0
6h	17.6±1.2	44.4±3.8	7.8±1.2	8.8±3.0	13.6±1.6	26.3±0.4	0	50.6±0.6	83.9±4.8
6i	31.6±2.8	40.6±2.9	10.5±3.4	15.0±3.1	11.5±3.1	3.3±7.1	17.2±4.3	90.2±0.3	90.8±1.4
6j	23.5±1.5	63.3±3.9	33.3±5.1	2.9±3.1	18.2±0.5	0	7.3±0.7	73.8±4.4	91.6±3.6
6k	47.4±0.2	40.6±4.5	3.3±3.6	20.0±4.0	11.5±3.2	4.9±3.8	3.4±1.9	17.1±3.7	90.1±0.1
6l	15.8±2.4	42.5±3.6	10.3±2.5	5.5±3.3	7.7±2.1	27.9±4.2	17.2±2.9	81.0±1.7	79.5±3.4
6m	10.5±4.9	55.3±4.6	10.1±0.7	15.1±2.5	5.8±0.4	6.6±0.1	13.8±4.2	57.1±2.6	93.9±3.5
6n	10.5±4.1	63.8±4.9	3.3±3.9	5.4±4.9	3.8±3.4	8.2±0.4	17.2±3.7	82.2±3.6	95.4±4.2
Thifluzamide	89.5±2.8	86.3±0.6	20.1±1.3	80.0±3.2	23.1±1.9	27.9±2.9	27.6±0.3	76.6±2.2	90.1±4.4
Fluxapyroxad	38.0±1.9	100.0	100.0	0	0	38.4±0.9	0	33.6±6.2	88.2±0.9
Isopyrazam	27.0±2.6	64.0±2.3	48.0±1.1	0	0	50.3±4.6	0	38.1±5.8	84.0±4.3

[a]Values are the mean ± standard deviation (SD) of three replicates

[b]*A. s*: *Alternaria solani*; *B. c*: *Botrytis cinerea*; *C. a*: *Cercospora arachidicola*; *G. z: Gibberella zeae; P. i*: *Phytophthora infestans* (Mont) de Bary; *P. p*: *Physalospora piricola*; *P. s*: *Pellicularia sasakii*; *R. c*: *Rhizoctonia cerealis*; and *S. s*: *Sclerotinia sclerotiorum.*

Table 2. Chemical Structures and Fungicidal Activities with EC_{50} against *S. sclerotiorum, B. cinerea* and *R. cerealis* of the Target Compounds

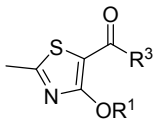

Compd	R^1	R^3	EC_{50}[a] (mg/L)		
			S. sclerotiorum	*B. cinerea*	*R. cerealis*
5a	CH_3	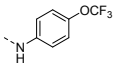	0.5±0.1	68.2±0.8	>100
5b	CH_3		14.1±0.2	77.5±1.0	55.5±2.1
5c	CH_3		20.0±0.3	26.7±0.5	108.5±6.8
5d	CH_3	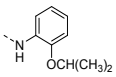	16.2±0.3	70.1±0.6	>100
5e	CH_3		35.0±0.7	>100	49.6±0.2
5f	CH_3	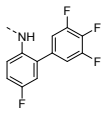	17.0±0.5	36.0±0.7	59.4±0.5
5g	CH_3	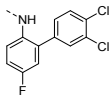	14.7±0.1	81.9±2.3	29.7±0.2
5h	CH_3	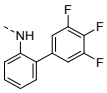	>100	>100	>100
5i	CH_3	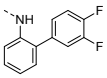	2.6±0.1	59.1±1.0	5.0±0.4
5j	CH_3	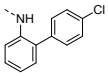	8.3±0.1	12.7±0.3	7.9±0.1
5k	CH_3		>100	>100	97.5±1.0
5l	CH_3		>100	>100	60.0±0.5
5m	CH_3		29.0±0.3	11.3±0.1	27.1±0.4
5n	CH_3		12.3±0.3	21.7±0.4	16.4±0.3

5o	CH_3	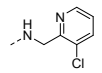	33.7±0.6	>100	21.7±1
5p	CH_3	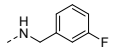	23.4±0.4	11.3±0.3	>100
5q	CH_3	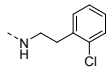	18.1±0.3	43.1±0.7	43.5±0.7
5r	Propargyl	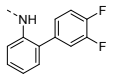	40.0±1.3	101.0±1.0	18.4±0.3
6a	OH	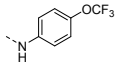	6.8±0.2	63.4±0.4	11.3±0.3
6b	OH	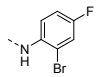	1.0±0.2	24.3±1.0	30.0±0.5
6c	OH		1.3±0.1	40.0±0.5	13.2±0.1
6d	OH	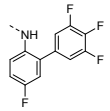	9.8±0.3	33.6±0.3	4.7±0.2
6e	OH	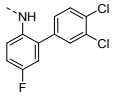	10.6±0.1	79.4±1.0	81.1±0.8
6f	OH	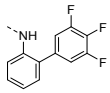	2.3±0.1	33.6±0.5	1.2±0.1
6g	OH	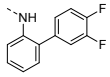	0.6±0.1	42.3±0.2	6.2±0.3
6h	OH	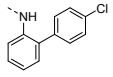	14.0±0.4	64.5±0.9	68.3±0.1
6i	OH		13.0±0.4	128.2±3.2	9.8±0.1
6j	OH		8.0±0.4	39.7±0.2	143.5±6.4
6k	OH		1.9±0.2	>100	>100
6l	OH	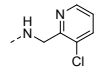	34.4±0.5	>100	25.8±0.4
6m	OH	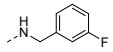	4.8±0.3	42.4±0.2	40.3±0.3
6n	OH	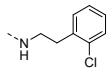	11.0±0.4	13.1±0.1	30.9±0.2
Trifluzamide			4.3±0.1	10.4±0.2	22.1±0.3

[a]Values are the mean ± standard deviation (SD) of three replicates

Table 3. *In vivo* Activity of Target Compounds against *S. sclerotiorum* Infected *Brassica napus* L. Leaves.[a]

		Protective activity		Curative activity		Inactivation activity	
Compd	(mg/L)	Diameter of lesions (cm)	Control efficacy (%)	Diameter of lesions (cm)	Control efficacy (%)	Diameter of lesions (cm)	Control efficacy (%)
5i	2.0	2.47±0.26	0.0	1.40±0.07	56.7	2.77±0.41	15.0
6c	2.0	0.83±0.05	75.4	2.10±0.18	23.1	0.93±0.19	83.9
6f	2.0	2.17±0.29	0.0	1.60±0.39	47.1	2.30±0.37	32.6
6g	2.0	1.00±0.16	67.3	2.22±0.16	17.3	0.87±0.17	86.1
TF[b]	5.0	2.70±0.24	0.0	2.27±0.26	14.9	0.70±0.08	92.5
TF	10.0	2.65±0.27	2.3	1.80±0.01	43.0	0.57±0.05	97.4
CK	0.0	2.03±0.44	-	2.58±0.19	-	3.17±0.12	-

[a] Values are the mean ± standard deviation (SD) of three replicates.

[b] Trifluzamide

Table 4. SDH Enzymatic Inhibition Activity (IC_{50})

Compd	**5i**	**5j**	**6c**	**6f**	**6g**	Thifluzamide
IC_{50}[a] (mg/L)	2.27±0.47	10.77±2.20	0.89±0.15	2.28±0.55	0.56±0.12	0.55±0.15

[a] Values are the mean ± standard deviation (SD) of three replicates.

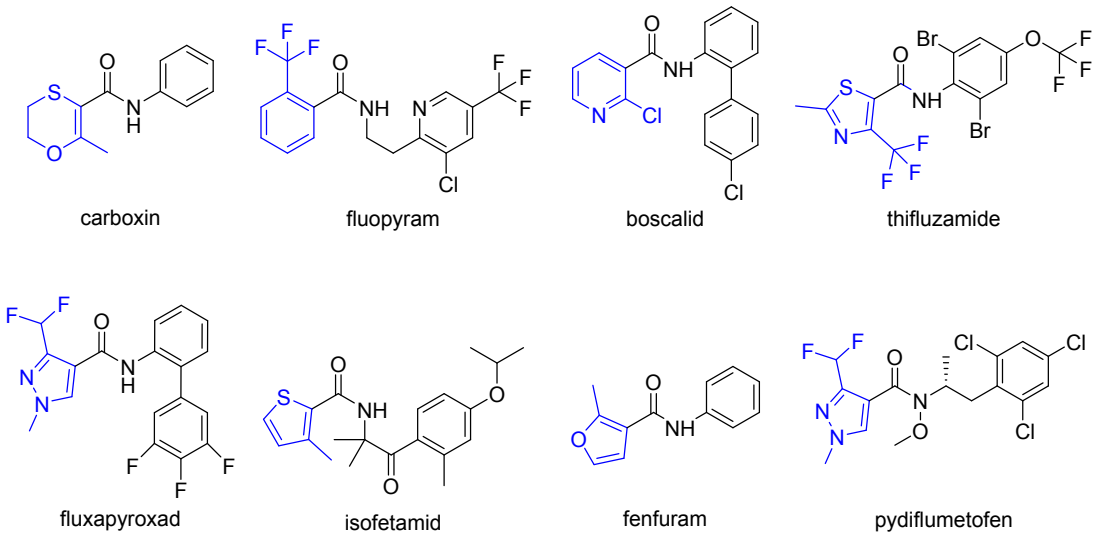
carboxin
fluopyram
boscalid
thifluzamide
fluxapyroxad
isofetamid
fenfuram
pydiflumetofen

Figure 1.

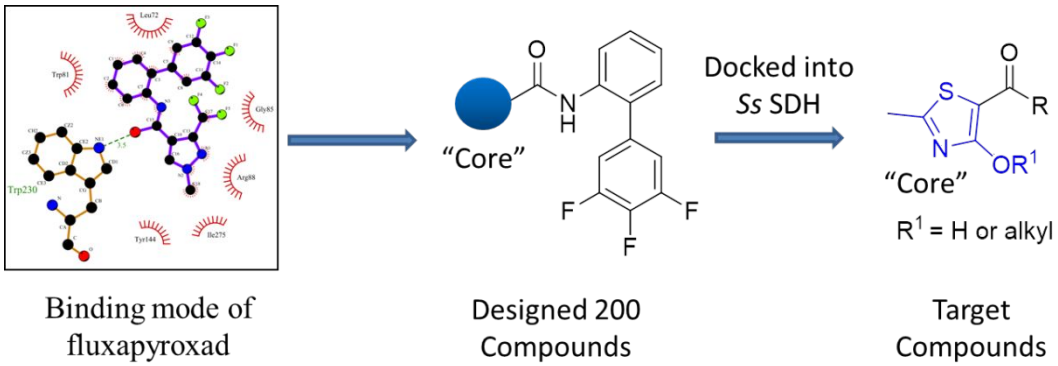
Docked into
Ss SDH
"Core"
"Core"
R1 = H or alkyl
Binding mode of fluxapyroxad
Designed 200 Compounds
Target Compounds

Figure 2.

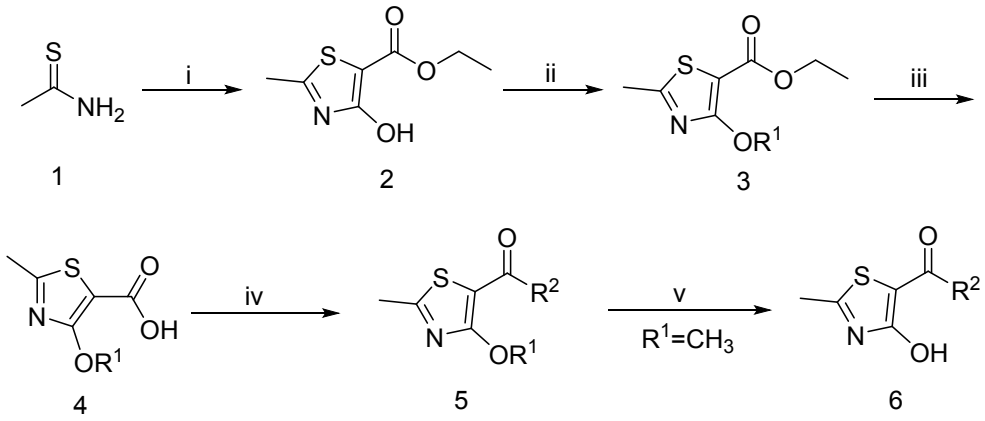
S
NH2
i
O
S
N
OH
O
ii
O
S
N
OR1
O
iii
1
2
3
S
N
OR1
O
OH
iv
O
S
N
OR1
R2
v
R1=CH3
O
S
N
OH
R2
4
5
6

Figure 3.

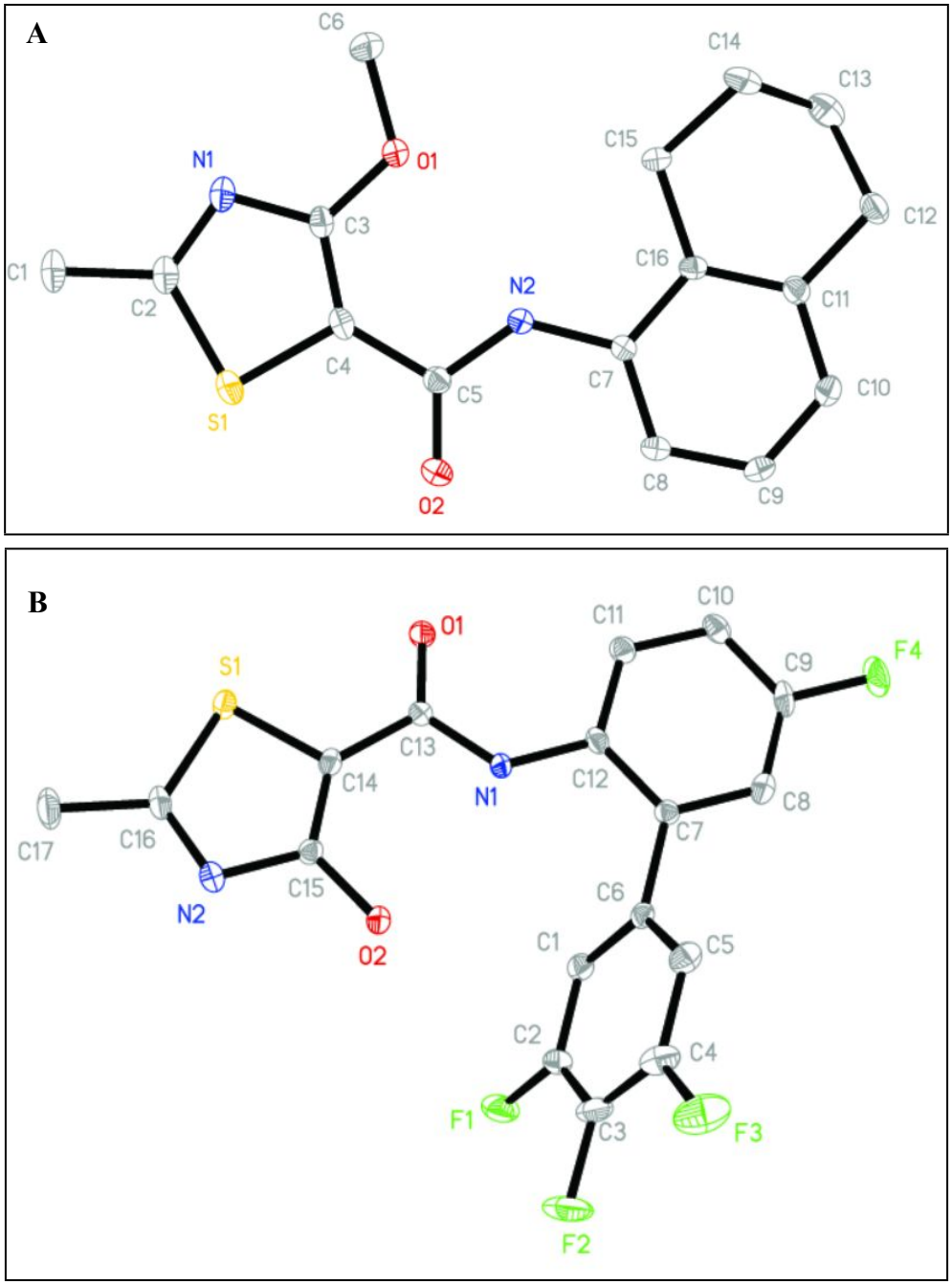
A
C6
O1
N1
C3
C1
C2
S1
C4
C5
O2
N2
C7
C14
C13
C15
C12
C16
C11
C10
C8
C9
B
O1
S1
C13
C14
N1
C17
C16
C15
N2
O2
C11
C10
C9
F4
C12
C8
C7
C6
C1
C5
C2
C4
F1
C3
F3
F2

Figure 4.

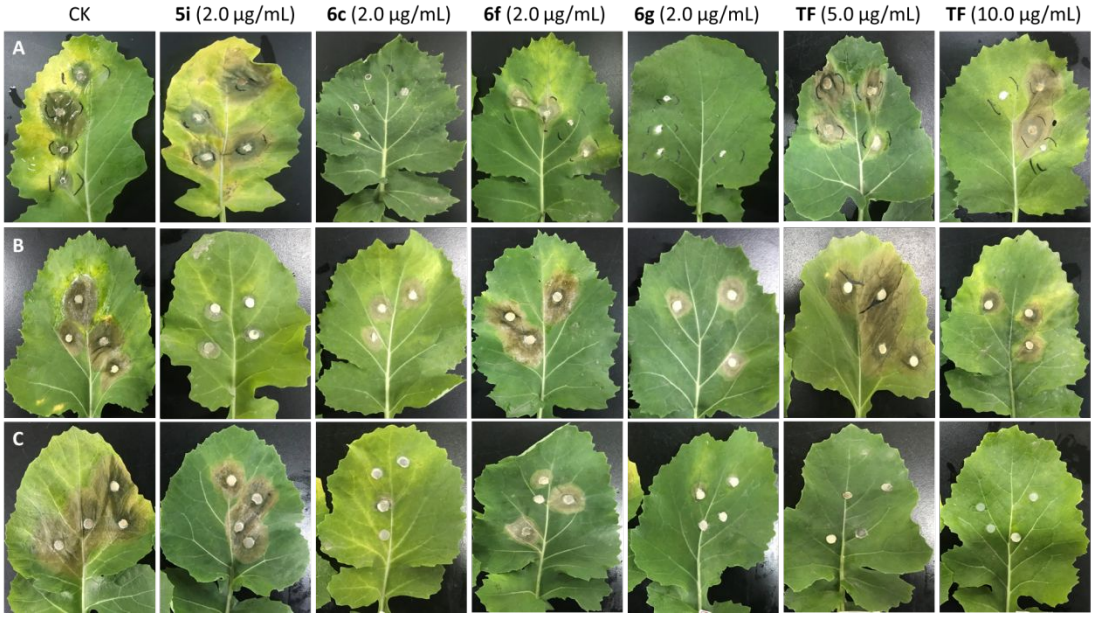
CK
5i (2.0 μg/mL)
6c (2.0 μg/mL)
6f (2.0 μg/mL)
6g (2.0 μg/mL)
TF (5.0 μg/mL)
TF (10.0 μg/mL)
A
B
C

Figure 5

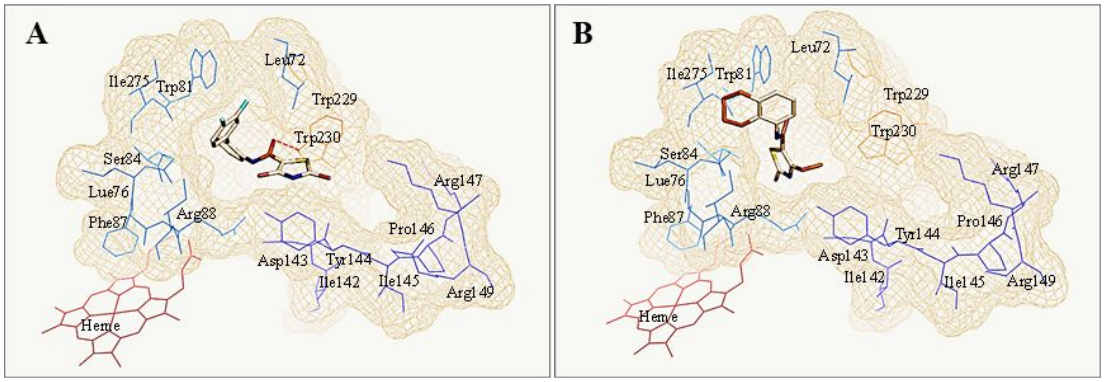
A
Ile275
Trp81
Leu72
Trp229
Trp230
Ser84
Lue76
Phe87
Arg88
Arg147
Pro146
Asp143
Tyr144
Ile142
Ile145
Arg149
Heme
B
Leu72
Ile275
Trp81
Trp229
Trp230
Ser84
Lue76
Phe87
Arg88
Arg147
Pro146
Tyr144
Asp143
Ile142
Ile145
Arg149
Heme

Figure 6.

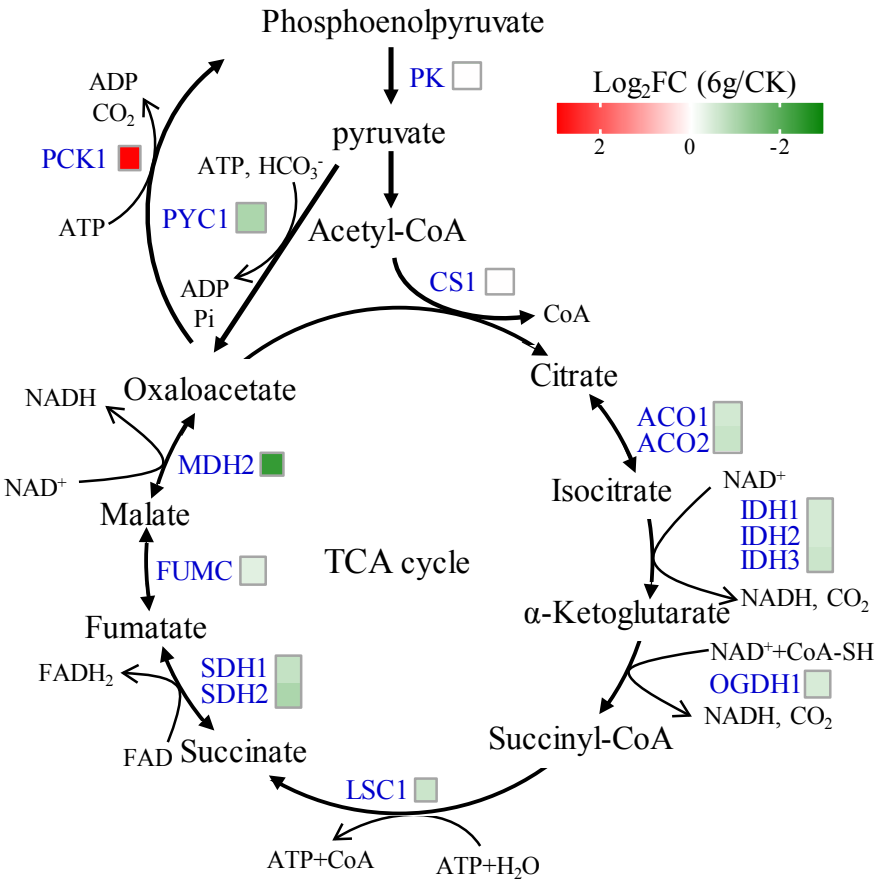
Phosphoenolpyruvate
PK
pyruvate
Log2FC (6g/CK)
2
0
-2
ADP
CO2
PCK1
ATP
ATP, HCO3-
PYC1
Acetyl-CoA
ADP
Pi
CS1
CoA
Citrate
NADH
Oxaloacetate
ACO1
ACO2
NAD+
MDH2
Malate
Isocitrate
NAD+
IDH1
IDH2
IDH3
NADH, CO2
FUMC
TCA cycle
α-Ketoglutarate
Fumatate
NAD+ +CoA-SH
OGDH1
NADH, CO2
FADH2
SDH1
SDH2
FAD
Succinate
Succinyl-CoA
LSC1
ATP+CoA
ATP+H2O

Figure 7.

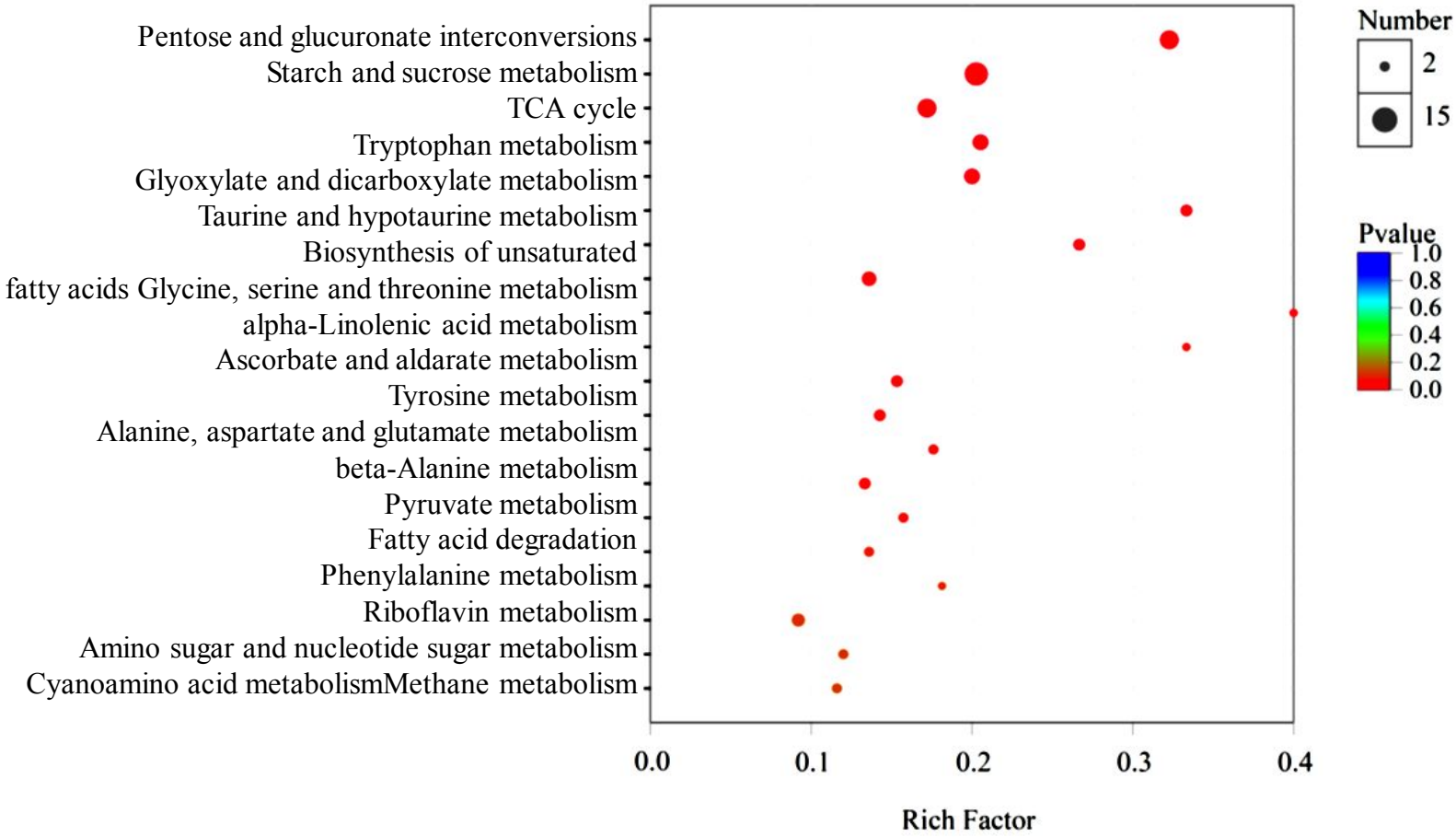
Pentose and glucuronate interconversions
Starch and sucrose metabolism
TCA cycle
Tryptophan metabolism
Glyoxylate and dicarboxylate metabolism
Taurine and hypotaurine metabolism
Biosynthesis of unsaturated
fatty acids Glycine, serine and threonine metabolism
alpha-Linolenic acid metabolism
Ascorbate and aldarate metabolism
Tyrosine metabolism
Alanine, aspartate and glutamate metabolism
beta-Alanine metabolism
Pyruvate metabolism
Fatty acid degradation
Phenylalanine metabolism
Riboflavin metabolism
Amino sugar and nucleotide sugar metabolism
Cyanoamino acid metabolismMethane metabolism
0.0
0.1
0.2
0.3
0.4
Rich Factor
Number
2
15
Pvalue
1.0
0.8
0.6
0.4
0.2
0.0

Figure 8.

Graphic for table of contents